

Real-time Motion Control of a Multi-degree-of-freedom Variable Reluctance Spherical Motor

Zhi Zhou

AT&T Bell Laboratories
Suite G020, 2000 Northeast Expressway
Norcross, GA 30071

Kok-Meng Lee

The George W. Woodruff School of Mechanical Engineering
Georgia Institute of Technology
Atlanta, GA 30332-0405

Abstract This paper presents high-precision control strategies and bearing support mechanisms for real-time motion control of a multiple degree-of-freedom (DOF) variable-reluctance (VR) spherical motor. In particular, a resultant magnetic force model is derived which, along with the torque model, is used to develop a reaction-free control strategy to establish a non-contact support mechanism through magnetic levitation to achieve high performance motion. An equivalent angle-axis based control is also designed and implemented for real-time applications. The designed control strategy only requires limited knowledge of system dynamics, therefore is robust and practical. A look-up table based on-line nonlinear optimization scheme is devised to facilitate the control strategy for a prototype VR spherical motor. Control experimental results verify the reaction-free control strategy and demonstrate the motion capability of the multi-DOF VR spherical motor. The concepts, methodologies, and experimental techniques developed in the paper establish an essential analytical and engineering basis for real-time motion control of VR spherical motors.

1 Introduction

Many advanced manufacturing processes require smooth, high-precision, and/or high-speed robotic manipulations in three dimensional space. Existing robotic manipulators are usually constructed using single-axis motors in series and/or parallel connected by linkages to realize a three dimensional motion. Such configuration, however, tends to be larger in size and mass; usually have decreased motion accuracy due to mechanical deformation, friction and backlash of gears and linkages; and may result in physical singularities in workspace which is a major obstacle in obtaining uniform and high-precision motion.

For high-precision robotic manipulations, it is desired that the gears and linkages be eliminated and the multiple single DOF motors replaced by one multi-DOF actuator.

One attractive mechanism that offers potential solution to the problem is the VR spherical motor which is capable of performing three dimensional motion in a single joint. The VR spherical motor possesses several advantages over the conventional and current robotic actuators including its relatively simple and compact structure and large range of continuous motion with uniform resolution. These attractive features offer the multi-DOF device significant potential in applications such as coordinate measuring, high-speed plasma, and laser cutting where a high-precision motion and fast dynamic response are crucial to the system performance and product quality.

Lee *et al.* [1] presented the dynamic modeling of a VR spherical motor in terms of rotor dynamics and a torque model. The rotor dynamics have been expressed in terms of *XYZ* Euler angles and the actuating torques. The torque model of a current-controlled VR spherical motor has been derived in a rotor-fixed Cartesian coordinate. For a set of specified currents at a given rotor orientation, the torques of a VR spherical motor can be uniquely predicted by its forward torque model. The inverse problem of the torque model, that is, to find a set of input currents such that they generate a desired torque at a particular orientation, is characterized by its nonlinearity and multiplicity of the solutions, which offers the flexibility in control. The solution to the inverse problem has been formulated as an optimization problem by Lee *et al.* in [1]. The generalized reduced gradient (GRG) method [2] has been suggested to solve the optimization problem. Lee *et al.* also addressed a computed-torque control strategy which illustrated the control concept of the VR spherical motor. Their approach, however, did not take into account of the unbalanced magnetic force and the resultant friction which has significant effect on motion control performance especially at low speeds.

Zhou and Lee [3] have presented a methodology for characterization and design optimization of multi-DOF VR spherical motors. In particular, a maximum torque formula has been derived to predict the torque output capability, to

numerically verify the non-singularity property, to provide desirable objective function for design optimization, and to determine characteristic specifications of the VR spherical motor. Typical characteristic specifications of the VR spherical motor prototype have been determined. These characteristic specifications serve as constraints in motion control law design of the VR spherical motor.

Previous research has demonstrated the basic principle and design methodology of the VR spherical motor by focusing on modeling the electromagnetic interaction (torque model). To advance the development, however, many key issues need to be further investigated. These issues are (1) reduction or elimination of internal friction to achieve high resolution motion, and (2) control strategy development and its real-time implementation. The thrust of this paper is to study analytically and experimentally the above-mentioned issues. The major contributions of this paper research are two-fold: (1) The paper presents a reaction-free control strategy to magnetically levitate the rotor in order to reduce the internal friction and enhance the system performance without complicating the system structure. The magnetic non-contact supporting mechanism is achieved by control strategy design and dynamic modeling. The modeling of the resultant force serves as a key step toward the control law design, and the reaction-free control law designed as a basis for the magnetic levitation mechanism. The new concept development of permeance model with variable air-gap and its experimental determination play critical roles in implementation of the reaction-free control strategy. (2) The paper derives innovative practical algorithms for implementing in real-time the control strategy. An equivalent angle-axis based control and optimization system demonstrates the ability of real-time applications of the multi-DOF spherical motors. The work established in this paper research provides better insights into design, manufacture, and control of unusual robotic actuators.

The remaining paper is divided into three sections. Section 2 outlines dynamic modeling, develops reaction-free control strategy and demonstrates the idea of magnetic levitation to reduce the internal friction and thus enhance the performance of an actuator. Section 3 derives and implements practical control and optimization techniques for real-time control applications of the VR spherical motor. A number of motion control experiments are performed and the results presented. Finally, conclusions of this work are given in section 4.

2 Reaction-free Control Strategy via Magnetic Levitation

This section investigates a reaction-free control strategy and associated dynamic modeling for the VR spherical motor in order to reduce the bearing friction thus to achieve high-precision motion. Especially, the section derives an analytical model describing the resultant magnetic force which is required in designing the reaction-free control strategy. Illustrative experimental results show that the reaction-free control strategy reduces the bearing friction and improves

the system performance.

2.1 Magnetic Torque Generation and the Resultant Magnetic Force

The magnetic force balancing or the elimination of the bearing friction requires an explicit model of the magnetic force. In order to model the magnetic force, the VR spherical motor has been extended conceptually from three DOF to six DOF by allowing the rotor to translate. It has been derived based on the principle of conservation of energy and geometry differential that the generated magnetic torque and resultant force can be modeled as follows [4]:

$$T_{mk} = \frac{1}{2} \mathbf{u}^T \mathbf{A}_k \mathbf{u}, \quad (1)$$

$$F_{mk} = \frac{1}{2} \mathbf{u}^T \mathbf{B}_k \mathbf{u} \quad (2)$$

where $k = 1, 2, 3$, and

$$\mathbf{u} = [M_{s1}, M_{s2}, \dots, M_{sm_s}]^T \in \mathbf{R}^{m_s},$$

$$\mathbf{A}_k = \sum_{i=1}^{m_s} \left(\sum_{j=1}^{n_r} \frac{\partial P(\varphi, d_{ij})}{\partial \varphi} \Big|_{\varphi=\varphi_{ij}} (\vec{e}_{ij} \bullet \vec{e}_k) \right) ac_i \quad (3)$$

$$\mathbf{B}_k = \sum_{i=1}^{m_s} \left(\sum_{j=1}^{n_r} \frac{\partial P(\varphi_{ij}, d)}{\partial d} \Big|_{d=d_{ij}} (\vec{e}_{ij} \bullet \vec{E}_k) \right) ac_i \quad (4)$$

$$ac_i = (\mathbf{a} - \mathbf{c}_i)(\mathbf{a} - \mathbf{c}_i)^T,$$

$$\mathbf{c}_i = [0, \dots, 0, 1, 0, \dots, 0]^T,$$

$$\mathbf{a} = [a_1, a_2, \dots, a_i, \dots, a_{m_s}]^T,$$

$$a_i = \sum_{j=1}^{n_r} P_{ij} / \left(\sum_{i=1}^{m_s} \sum_{j=1}^{n_r} P_{ij} \right) \sum_{i=1}^{m_s} a_i = 1$$

and where the permeance function P_{ij} and the matrices \mathbf{A}_k and \mathbf{B}_k are functions of both orientation and translation of the rotor. The permeance function P_{ij} can be determined experimentally.

2.2 Reaction-free Motion Control

The objective of reaction-free control strategy is to balance the resultant force, while generating the required torque for a desired rotation, so that the rotor is magnetically levitated rendering the friction between the rotor and the bearings negligible. Due to the elimination of the friction, the VR spherical motor system with reaction-free control strategy will have a high-precision torque control, a smooth motion, and a fast dynamic response.

The control of a VR spherical motor consists of two parts, force/torque control laws and solution to inverse torque/force models. The torque and force required to generate a specified path are referred to as the torque and force control laws. The desired path is specified as $\mathbf{q}_d = [\mathbf{q}_{dT}, \mathbf{q}_{dF}]^T = [\psi_d, \theta_d, \phi_d, 0, 0, 0]^T$, where the Euler angles ψ , θ , and ϕ are functions of time. The force control law $\mathbf{F} = \mathbf{M}_F \dot{\mathbf{q}}_{dF}$ will guarantee that the linear

displacement tracking error approaches to zero asymptotically. Since $\mathbf{q}_{dF} = \mathbf{0}$, the reaction-free force control law is determined by

$$F_{m1} = 0, \quad F_{m2} = 0, \quad F_{m3} = m_r g$$

where the magnetic force component in Z direction will balance the gravity of the rotor.

The torque control law can be designed by an equivalent angle-axis based approach as follows. It has been known that the rotation of a 3D rigid body can be represented by equivalent angle-axis [5]. For the VR spherical motor, once current and desired orientations are known, the equivalent axis and angle can be calculated so that if the rotor (body-fixed) frame rotates about the axis by the amount of the angle, the rotor frame will reach the target orientation. The equivalent axis determines the driving torque direction, while the magnitude of the driving torque should be directly proportional to the equivalent angle in order to reach the target position as quickly as possible. The actual time taken to get to the target position depends upon the control gain. Theoretically, the larger is the control gain, the faster the rotor frame reaches the target position. Practically, however, the maximum possible torque output of the actuator is limited due to the rated (maximum) current allowed through the stator coils. Furthermore, because of system inertia larger driving torque may cause significant overshoot. To avoid large overshoot or keep the overshoot within a reasonable range, the gain must be constrained, and a velocity feedback can be introduced. Intuitively when the angular velocity is large, the driving torque should be reduced to prevent from overshoot. The control strategy described above can be written as

$$\vec{T}_m = (K_1\theta + K_2\dot{\theta})\vec{K}_e \quad (5)$$

where K_1 and K_2 are the position and velocity control gains, respectively, and can be determined experimentally; θ and $\dot{\theta}$ are equivalent angle and its time derivative; and \vec{K}_e specifies the equivalent axis. Equation (5) is in fact equivalent to a proportional control law with velocity feedback in terms of the equivalent angle-axis. Compared with the computed torque control strategy [1], the equivalent angle-axis based control is physically intuitive and meaningful. Such designed control law has less requirement on dynamic model, therefore, it is easy to implement and computationally efficient. The trade-off of this control strategy, however, is that there is no analytical way to determine the control parameters, they must be tuned experimentally as will be discussed in Section 3.2.

The inverse force/torque models are defined here as to find the electrical inputs through the stator coils which would generate the required magnetic force and torque determined from the reaction-free control strategy, that is the solution to the following torque/force constraints.

$$\begin{aligned} \frac{1}{2}\mathbf{u}^T \mathbf{A}_1 \mathbf{u} &= T_{m1}, & \frac{1}{2}\mathbf{u}^T \mathbf{A}_2 \mathbf{u} &= T_{m2}, & \frac{1}{2}\mathbf{u}^T \mathbf{A}_3 \mathbf{u} &= T_{m3}, \\ \frac{1}{2}\mathbf{u}^T \mathbf{B}_1 \mathbf{u} &= 0, & \frac{1}{2}\mathbf{u}^T \mathbf{B}_2 \mathbf{u} &= 0, & \frac{1}{2}\mathbf{u}^T \mathbf{B}_3 \mathbf{u} &= m_r g \end{aligned}$$

where T_{mk} ($k = 1, 2, 3$) is determined from the torque control law (5). The force/torque models can be solved

for a unique solution to minimize the power consumption. In practical implementation of this optimization algorithm, the torque and force constraints can be combined via penalty factors with the objective function such as the consumed electrical power. Different penalty factors can be used as the weights of the torque and force errors to specify the different priority on the corresponding torque and force constraints.

3 Motion Control Experiment

This section presents a practical real-time motion control algorithm for the innovative six DOF VR spherical motor. Experimental results validate the designed control strategy, and demonstrate the potential of the VR spherical motor for a wide variety of high performance motion control applications.

3.1 Experimental Investigation of the Reaction-free Control Strategy

The experimental test-bed used to verify the analytical magnetic force model and to validate the reaction-free control strategy is shown in Figure 1. In this experimental setup, the rotor is allowed to translate; in other words, the motor has six degrees of freedom. However, only the three DOF rotation are used in motion realization. The three DOF translation are used to levitate and center the rotor for non-contact magnetic support of the mechanism.

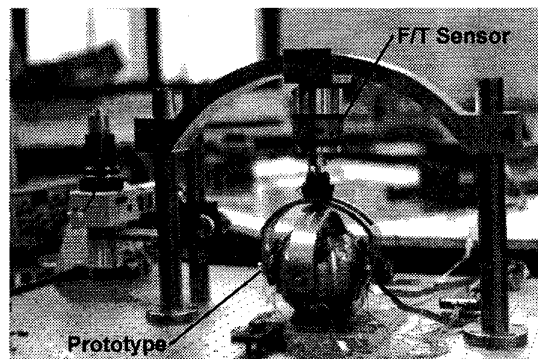


Figure 1: Experimental Setup

Theoretical analysis shows that reaction-free control strategy can be used to achieve high precision motion of the VR spherical motor. For comparison with the three DOF case where the unmodeled magnetic force was balanced by the transfer bearings, a number of torque/force tests at rotor orientation $(0^\circ, 0^\circ, 0^\circ)$ have been performed. Figure 2 shows the torque and force measurements with various specified torques in z direction in the cases of with or without the force model, respectively. The magnitude of the desired torques was limited in the experiments to be less than $0.1 Nm$ in order to avoid the magnetic saturation of the magnetic circuit. One observes from Figure 2 that the

overall resultant force acting on the rotor, particularly the force component in Z direction, is reduced when the magnetic force model is taken into consideration in the motion control of the motor. As shown in Figure 3, within the range of desired/actual torque less than 0.1 Nm , the torque errors accounting for the effect of the force model are, in general, smaller or in the same order of magnitude than that of the case without the force model within the measurement tolerance of the F/T sensor. Further reduction of the torque error of using the force model is expected for torque tests with larger desired torque, because of a more significant reduction of the magnetic force.

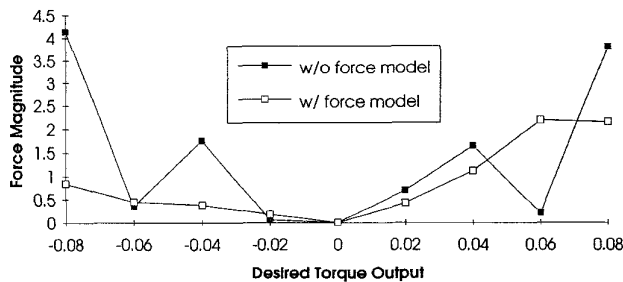


Figure 2: Resultant Magnetic Force

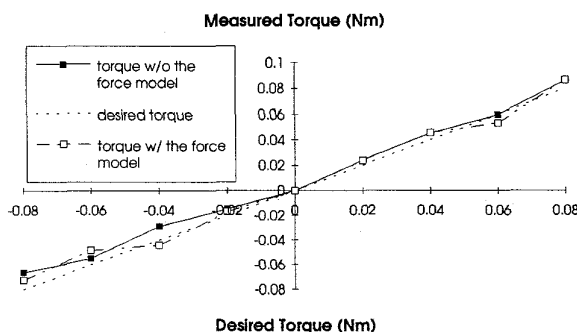


Figure 3: Magnetic Torque Errors

3.2 Real-time Control Applications

The experimental test-bed for real-time control applications is similar to the one shown in Figure 1 except the motor is inverted here in order to track a designed motion pattern plotted on an experimental platform. The position and velocity control gains used in the experiment are $K_1 = 9 \text{ Nm/rad}$ and $K_2 = -6 \text{ Nm} \cdot \text{s/rad}$, respectively. All the experiments are performed without any external load applied to the motor. However, the internal load introduced by the mechanical housing of the encoder system is compensated through a load compensation. A constant gain $K_l = 2$ is chosen as a weighting factor for the load compensation. The maximum control current, which serves as a constraint in control law implementation, is limited to 3 Amps considering the electrical and thermal ratings of the

stator coils as well as the magnetic saturation of the stator cores. A look-up table of 972 points that partitions the VR spherical motor workspace with five degree intervals is used as initial predictions of the nonlinear control input optimization. The penalty function used in the optimization is chosen to be 10^4 .

The objective of position control of the VR spherical motor is to control the rotor shaft from an arbitrary initial position to a desired target position. Two sets of experiments are performed to illustrate the motion ability of the VR spherical motor. They are motion realization experiments with or without spin motion. The experiment results of the first set of experiments, namely the motion without spin, is recorded in terms of XYZ Cartesian coordinates, while the motion with spin is documented in ZYZ Euler angles. Various position control tests with different target and/or initial positions are conducted in the experiment.

Typical position control experimental results are plotted in Figures 4 ~ 9. And the performance characteristic parameters, such as steady-state error, e_{ss} (normalized), maximum overshoot, M_s (% or degrees), and settling time, t_s (time steps) are computed and listed in Tables 1 and 2. The 2% criterion is used in calculating the settling time in order to measure the response time. For each position control experiment, the actual path from a starting position (marked with "*" in the figures) to an ending position (marked with "o" in the figures) is plotted in 3D space. And the orientation components, either X, Y, Z , coordinates or ZYZ Euler angles are graphed in planner (2D) planes. As shown in the 3D plots, the motion of the controlled VR spherical motor reached the target positions with a reasonable position error. Most of the 2D response plots of the position components, as shown in Figures 5, 7, 8, and 9, exhibit second-order like system behavior. The system performance is analyzed in Tables 1 and 2. As shown in the tables, the steady-state error corresponding to all the cases are small, indicating that the device is able to reach the specified target position within the workspace with a tolerable error.

Compared Table 2 with Table 1, one found that the motions can be ranked with maximum overshoot in ascending order as, pure spin motion, plane motion (in $X - Z$ or $Y - Z$ planes) with no spin, 3D motion with no spin, and 3D motion with spin. The main source for the relative large overshoot is believed to come from the stiction and friction introduced by the housing of the encoder system. Due to the configuration of the encoder housing, the two guides have little effect on spin motion, therefore the overshoot of the spin motion is the smallest. In $X - Z$ or $Y - Z$ plane motions, only one guide has effect on the motion, and the load force imposed by the effective guide is always perpendicular to the rotor shaft and tangential to the path of motion. So that the overshoot in this case is moderate. In arbitrary 3D motions, the two guides both contribute to the relative larger overshoot due to larger friction and stiction and the resultant friction and/or load force that is no longer alien along the direction of motion, furthermore, it varies at different rotor orientation. The 3D motion with spin is the most general and complicated case for the exper-

imental setup. All the above discussed factors contribute to the largest time response overshoot.

The settling time is computed from the data which result the plots in Figures 4 ~ 9, the results are also given in Tables 1 and 2 in terms of time steps. The average control loop frequency of the system is about 12.5 Hz, in other words, each time step counts for $T = 1/12.5 = 0.08$ seconds. One observes from Tables 1 and 2 that the responses which exhibit large maximum overshoot took longer to settle, and the ones with small overshoot have shorter settling time. This result agrees, in general, with theoretical analysis. Also, notice that the actual settling time depends on the distance to travel from a starting point to an ending point, or the magnitude of input. More experimental results show that the system performance depends on specified starting and target positions due to the nonlinear dynamics of the VR spherical motor.

Table 1: Performance at Typical XYZ Positions

		(0.0024, 0.3114, 0.9503)	(-0.3644, 0.4155, 0.8334)
		↓	↓
		(-0.0025, -0.0151, 0.9999)	(-0.0464, 0.0414, 0.9981)
e_{ss}	X	-0.0025	-0.0464
	Y	-0.0151	0.0414
	Z	-0.0001	-0.0019
M_s	X	0.0000	6.7100
	Y	27.650	27.000
	Z	0.0000	0.2200
t_s	X	0	7
	Y	5	5
	Z	1	2

4 Conclusions

This paper has presented recent developments on control and modeling of an innovative VR spherical motor developed at Georgia Institute of Technology. A resultant magnetic force model has been derived which, along with the

Table 2: Performance at Typical ZYZ Positions

		(-0.22, 0.00, 46.30)	(-0.07, 0.36, -0.50)
		↓	↓
		(0.14, 1.15, 7.27)	(1.08, -7.13, -84.24)
e_{ss}	Z ₁	0.14	1.08
	Y	1.15	-7.13
	Z ₂	7.27	5.76
M_s	Z ₁	3.88	6.70
	Y	5.69	1.08
	Z ₂	0.00	0.08
t_s	Z ₁	12	49
	Y	13	55
	Z ₂	10	34

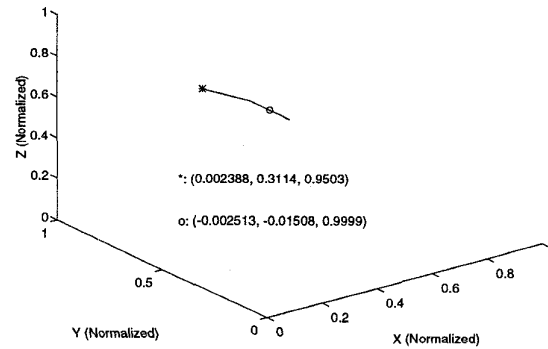


Figure 4: 3D XYZ Plot: (0.0024, 0.3114, 0.9503) → (-0.0025, -0.0151, 0.9999)

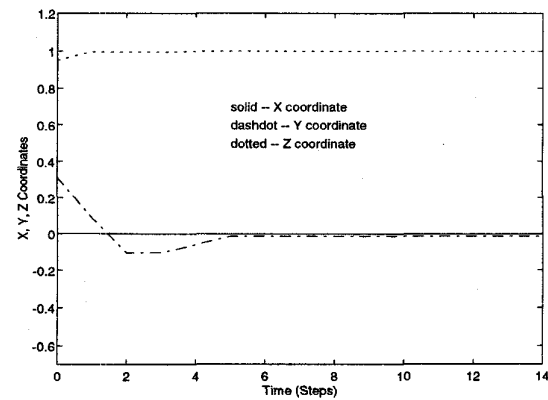


Figure 5: 2D XYZ Plot: (0.0024, 0.3114, 0.9503) → (-0.0025, -0.0151, 0.9999)

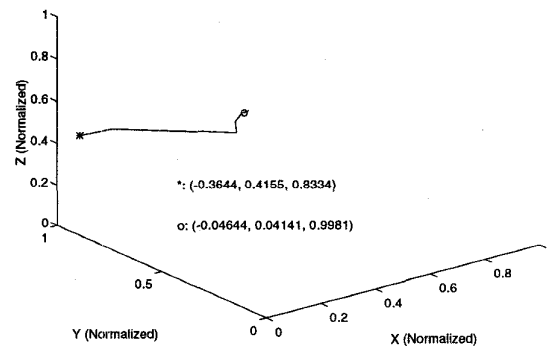


Figure 6: 3D XYZ Plot: (-0.364, 0.415, 0.833) → (-0.046, 0.041, 0.998)

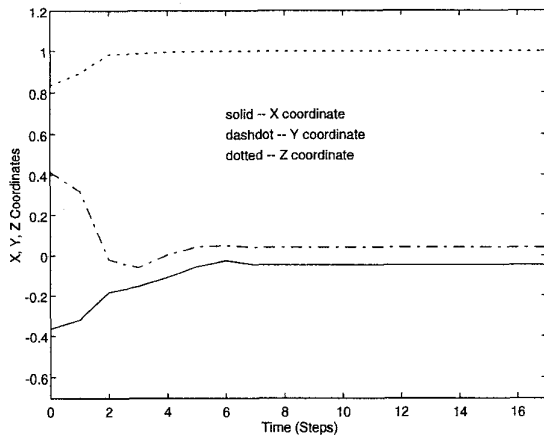


Figure 7: 2D XYZ Plot: $(-0.364, 0.416, 0.833) \rightarrow (-0.046, 0.041, 0.998)$

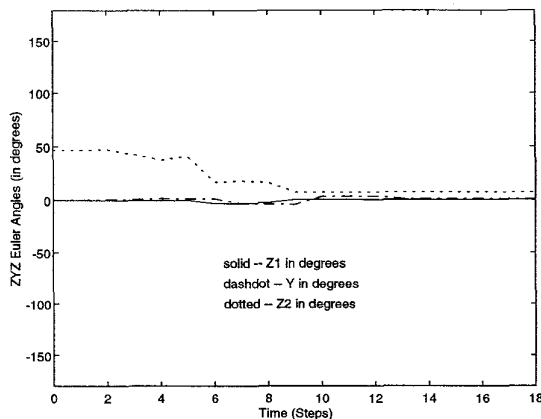


Figure 8: 2D ZYZ Plot: $(-0.22, 0, 46.3) \rightarrow (0.14, 1.15, 7.27)$

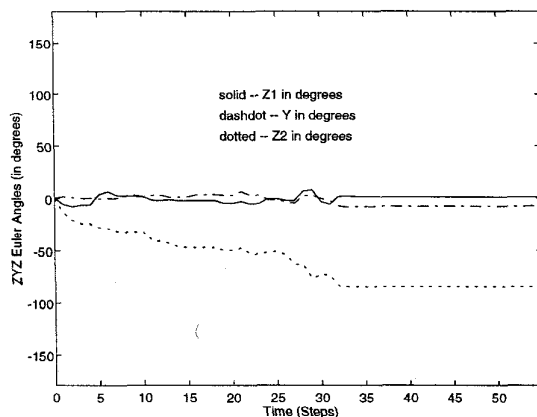


Figure 9: 2D ZYZ Plot: $(-0.07, 0.36, -0.5) \rightarrow (1.08, -7.13, -84.24)$

torque model, completes the dynamic modeling of the VR spherical motor. Six degrees of freedom VR spherical motor has been conceptualized by allowing the rotor to translate. The concept development allows a reaction-free control strategy be designed to magnetically levitate the rotor so that a non-contact support mechanism is established without additional system complication. As a result of the implementation of the reaction-free control strategy, high performance motion is achieved through the substantial reduction of the internal friction inherent to most driving mechanisms. The translation of the VR spherical motor leads to a new concept of permeance model with variable air-gap that is a function of both rotor orientation and translation. The permeance model has been determined experimentally.

Practical implementation techniques have been developed for real-time control applications. An equivalent angle-axis based control has been designed and implemented. The control strategy designed requires only limited knowledge of the system dynamics, thus physically intuitive and practically useful. A look-up table based on-line nonlinear optimization scheme has been taken to address practical implementation issues in control input optimization. A typical look-up table has been generated and implemented along with the GRG optimization algorithm. Various motion control experiments have been performed and results analyzed. Experimental results verified the control strategies and demonstrated the motion capability of the multi-DOF VR spherical motor. While the experiments illustrated the motion ability of the multi-DOF device, they also revealed constraints and limitations of the prototype design and provide insights for future design of the VR spherical motors.

References

- [1] Lee, K-M., Roth, R, and Zhou, Z., "Dynamic Modeling and Control of a Ball-joint-like Variable Reluctance Spherical Motor," *ASME Transactions on Dynamic Systems, Measurement and Control*, March, 1996.
- [2] Abadie, J, and Carpentier, J., "Generalization of the Wolfe Reduced Gradient Method to Case of Nonlinear Constraints," *Optimization*, Academic Press, 1969, pp. 37-47.
- [3] Zhou, Z. and Lee, Kok-Meng, "Characterization of a Three Degree-of-Freedom Variable Reluctance Spherical Motor," *Journal of Systems Engineering*, Special issue on Motion Control Systems, Vol. 4, No. 2, 1994, pp. 60-69.
- [4] Zhou, Z. and Lee, K-M., "A High Precision Torque Control of a Self Magnetically Levitated Six Degree-of-freedom Variable Reluctance Spherical Motor," *Dynamic Systems and Control* ASME Winter Annual Meeting, Nov., 1994, Chicago, IL, Vol. 2, pp. 775-780.
- [5] Craig, J. J., *Introduction to Robotics, Mechanics and Control*, Addison-Wesley Publishing Company, 1989.
- [6] Zhou, Z., *Real-time Control and Characterization of a Variable-Reluctance Spherical Motor*, Ph. D. thesis, Mechanical Engineering, Georgia Tech, 1995.